Theoretical and Experimental Study of the Melting Process of High-Density Polyethylene for Multidimensional Vibration Equipment

Guang-Sheng Zeng,[1,2] Jin-Ping Qu,[2] Yue-Jun Liu[1]

[1]*Key Laboratory of New Material and Technology for Package, Hunan University of Technology, Zhuzhou, Hunan Province 412007, China*
[2]*National Engineering Research Center of Novel Equipment for Polymer Processing, The Key Laboratory of Polymer Processing Engineering Ministry of Education, South China University of Technology, Guangzhou 510641, China*

Received 13 May 2010; accepted 13 July 2010
DOI 10.1002/app.33079
Published online 12 January 2011 in Wiley Online Library (wileyonlinelibrary.com).

ABSTRACT: A model for investigating the melting process under a vibration force field is presented. The key parameters of this model are as follows: the rotation of the screw and heat are supplied by the vibration force field for the material phase conversion. A multidimensional vibration desk (DWZD-500) and low-density polyethylene material were used to investigate the effect of the vibration parameters on the melting process. A comparison of the derived model and experimental results revealed that increasing the vibration parameters increased the melting mass. This study will serve as the theoretical basis to optimize the parameters of vibration extruders' processing polymers. © 2011 Wiley Periodicals, Inc. J Appl Polym Sci 120: 2912–2920, 2011

Key words: extrusion; melt; plastics; processing

INTRODUCTION

Most industrial extrusion machines plasticate input pellets and convert them to molten polymers. This is true of both conventional extruders and vibration-induced extruders. The single-screw extruder has been used widely to make thermoplastics since the 1930s. Since then, there have been many efforts to investigate and mathematically model the melting process. The first qualitative studies of melting in single-screw extruders were reported by Maddock[1] and Street[2] in the late 1950s. The first quantitative description of the melting model observed by Maddock and Street was developed by Tadmor.[3] In this model, the solid pellets are compacted in a solid bed, and a thin melt film forms between the solid bed and the barrel. Melting is assumed to occur primarily at the upper solid–melt interface. The melt added to the melt film through melting of the solid bed is dragged toward the leading flight flank. Most of this molten plastic accumulates in the melt pool at the leading flight flank. The melt pool pushes the solid bed against the trailing flight flank.

Another type of melting that has been observed by several workers describes separate, solid particles floating in a melt matrix. This melting model is termed *dispersed solid melting* and has been observed in twin-screw extruders, reciprocating single-screw compounders, and some regular single-screw extruders. Huang and Feng[4] performed a theoretical analysis of dispersed solid melting using a six-block model. Chris[5] presented a theoretical model for dispersed solid melting that allows closed-form solutions to the equations describing the problem. Qu and Zeng[13] established a melting model for vibration-force-field-induced extruders.

The vibration-force-field-induced extruder is a versatile and flexible device used in polymer processing and mixing. According to previous research,[14–18] the introduction of a vibration force field into the polymer extrusion process can increase the melting rate, decrease the length of the melting section, and reduce power consumption. Melting models describing the melting process of polymer materials have been a subject of focus because of its roles in providing a logical picture of the melting mechanics of polymers and providing aid in the design and optimization of polymer processing. Most of the

Correspondence to: G.-S. Zeng (guangsheng_zeng@126.com).

Contract grant sponsor: National Natural Science Foundation of China; contract grant numbers: 20074010, 10472034, 10590351.
Contract grant sponsor: National Natural Science Equipment Foundation of China; contract grant number: 20027002.
Contract grant sponsor: Department of Education of Hunan Province; contract grant number: 08C278.
Contract grant sponsor: Natural Science Foundation of Hunan Province; contract grant number: 09JJ6083.
Contract grant sponsor: Doctorate Foundation of South China University of Technology.

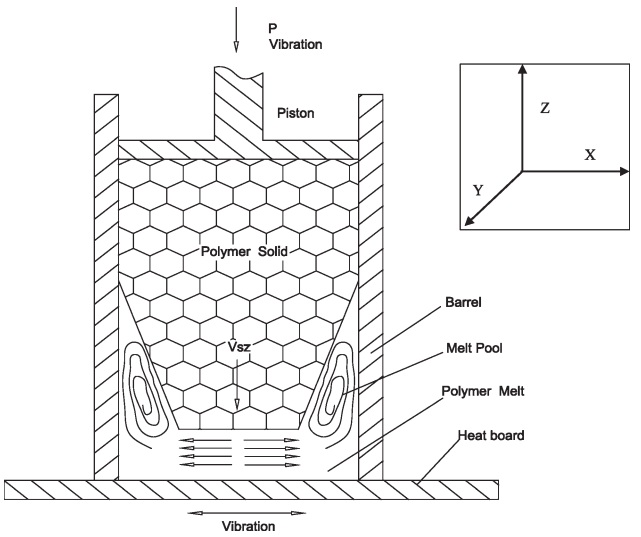

Figure 1 Melting model and coordinate.

current theoretical and experiment work in melting models has been devoted to the development of the melting process of polymers in a vibration-force-field-induced extruder. However, in vibration-force-field-induced extruders, the screw will vibrate as it rotates; hence, the vibration and the rotation should affect each other. Thus, it is difficult to study the separate effect of the vibration force field on the melting process. In this study, we designed a new experimental apparatus, and in this article, we present a new theory for the effects of the vibration force field on the melting process that allows closed-form solutions to the equations describing the problem. Predictions from the derived model are also compared to experimental results.

PHYSICAL MODEL FOR THE MELTING PROCESS

The physical model for the melting process is shown in Figure 1. A cylinder is filled with polymer pellets. The bottom of the barrel is a hot plate with a constant temperature (T_b) and can vibrate along the x direction at $A_2 \sin(\omega_2 t)$, where A_2 is the amplitude, ω_2 is the angle frequency, and t is time. A piston is used to apply a constant pressure (P) and can vibrate along the z direction at $A_1 \sin(\omega_1 t)$, where A_1 is the amplitude and ω_1 is the angle frequency.

The polymer pellets were first compacted into the cylinder (and create a solid bed) by the piston. The solid bed was assumed to be infinitely long along the z direction. A melt film formed between the solid bed and the hot plate. Melting occurred primarily at the solid–melt interface of the vibration force field. The melt added to the melt film from the solid bed was pushed toward the inner surface of the barrel and accumulated between the solid bed and the barrel and pushed the solid bed against the inner wall of the barrel to form a round melt pool between the solid bed and barrel. As the melting processing proceeded, the solid bed continued moving toward the melt film under a vibration force until the solid bed completely disappeared and the melt filled the entire barrel.

To simplify the deduction, the following assumptions were made:

1. To simplify the energy conservation equation, we assumed the wall of the barrel was adiabatic because the heat reached a balance when the system was in steady operation.
2. The heating part of the hot plate was controlled by a computer with an additional water cooling system in it, and thus, small deviations could be compensated for in a timely manner so that the temperature of the hot plate could be kept constant.
3. A great pressure was applied by the piston, so we assumed that the compression ratios of the melt and the solid were the same.
4. The polymer material melting temperature was T_m.
5. The melt was only generated at the solid–melt interface, which is shown in the experimental figure (Fig. 3, shown later), where the solid bed had a constant radius.
6. The mass and energy were all confined within the barrel; thus, it was a closed system.

ANALYTICAL MODEL FOR THE MELTING PROCESS

Continuous equation with a vibration force field

In this study, the physical melting model was a closed system, but the volume of the polymer varied with the vibration of the piston. Therefore, the compressibility of the polymer material was considered. The vibration equation for the piston was is follows:

$$\xi_1 = A_1 \sin(\omega_1 t) \tag{1}$$

where ξ_1 is the displacement of the piston.

As shown in Figure 1, the volume of the polymer material varied only along the z direction. If we let the mass of the material be M, the density (ρ) equation is

$$\rho = M/\pi R^2[H - A_1 \sin(\omega_1 t)] \tag{2}$$

where R is the radius of the barrel and H is the height of the polymer material. The substitution of eq. (1) into eq. (2) leads to eq. (3):

$$\frac{A_1\omega_1\cos(\omega_1 t)}{\pi R^2[H - A_1\sin(\omega_1 t)]} = -\left(\frac{\partial v_x}{\partial x} + \frac{\partial v_y}{\partial y} + \frac{\partial v_z}{\partial z}\right) \quad (3)$$

where v is the velocity of the material.

Momentum equation with a vibration force field

During this process, the material's flow will change its momentum. So, from the aspect of momentum conservation, we can research the rheological characteristics of the polymer melt. Also, because of the existence of the vibration field, the inertia term in the momentum equation cannot be ignored; if we let the vibration equation of the hot plate be

$$\xi_2 = A_2\sin(\omega_2 t) \quad (4)$$

where ξ_2 is the displacement of the hot plate, the following equations are obtained:

$$\rho\frac{dv_z}{dt} = \left(\frac{\partial \tau_{zz}}{\partial z} + \frac{\partial \tau_{zy}}{\partial y} + \frac{\partial \tau_{zx}}{\partial x}\right) + \rho g_z - \frac{\partial P}{\partial z} \quad (5)$$

$$\rho\frac{dv_x}{dt} = \left(\frac{\partial \tau_{xx}}{\partial x} + \frac{\partial \tau_{xy}}{\partial y} + \frac{\partial \tau_{xz}}{\partial z}\right) + \rho g_x\frac{\partial P}{\partial x} \quad (6)$$

and

$$\tau_{zz} = 2\eta\frac{\partial v_z}{\partial z} \quad (7)$$

$$\tau_{xx} = 2\eta\frac{\partial v_x}{\partial x} \quad (8)$$

$$\tau_{xz} = \eta\left(\frac{\partial v_x}{\partial z} + \frac{\partial v_z}{\partial x}\right) \quad (9)$$

$$\tau_{xy} = \eta\left(\frac{\partial v_x}{\partial y} + \frac{\partial v_y}{\partial x}\right) \quad (10)$$

$$\tau_{zy} = \eta\left(\frac{\partial v_z}{\partial y} + \frac{\partial v_y}{\partial z}\right) \quad (11)$$

where τ is the shearing stress, g is the acceleration of gravity, η is the apparent viscocity of melt.

Combining eqs. (4)–(11), we obtain

$$\frac{M}{\pi R^2[H - A_1\sin(\omega_1 t)]}\frac{dv_z}{dt} = \eta\left(\frac{\partial^2 v_z}{\partial y^2} + \frac{\partial^2 v_z}{\partial x^2}\right) + \frac{Mg_z}{\pi R^2[H - A_1\sin(\omega_1 t)]} \quad (12)$$

$$\frac{M}{\pi R^2[H - A_1\sin(\omega_1 t)]}\frac{dv_x}{dt} = \eta\frac{\partial^2 v_x}{\partial z^2} - \frac{\partial P}{\partial x} \quad (13)$$

Energy equation with a vibration force field

As stated earlier, under the impact of a vibration force field, the polymer is compressible; therefore, the volume distortion energy in the energy equation cannot be neglected, but the stress energy along the x and z directions due to volume distortion can be ignored. Moreover, if the temperature (T) of the polymer melt next to the hot plate is assumed to be constant and equal to that of the hot plate, the energy equation of the polymer melt can be obtained:

$$0 = \frac{\partial q_z}{\partial z} + T\left(\frac{\partial P}{\partial T}\right)_p\left(\frac{\partial v_x}{\partial x} + \frac{\partial v_y}{\partial y} + \frac{\partial v_z}{\partial z}\right) + \left\{\left[\tau_{xz}\left(\frac{\partial v_x}{\partial z} + \frac{\partial v_z}{\partial x}\right)\right] + \tau_{zy}\frac{\partial v_z}{\partial y}\right\} \quad (14)$$

where q_z is the heat flow.

Descending velocity of the solid bed

Combining the previous equations, we have

$$\begin{cases} \dfrac{A_1\omega_1\cos(\omega_1 t)}{\pi R^2[H - A_1\sin(\omega_1 t)]} = -\left(\dfrac{\partial v_x}{\partial x} + \dfrac{\partial v_y}{\partial y} + \dfrac{\partial v_z}{\partial z}\right) \\ \dfrac{M}{\pi R^2[H - A_1\sin(\omega_1 t)]}\dfrac{dv_z}{dt} = \eta\left(\dfrac{\partial^2 v_z}{\partial y^2} + \dfrac{\partial^2 v_z}{\partial x^2}\right) + \dfrac{Mg}{\pi R^2[H - A_1\sin(\omega_1 t)]} \\ 0 = \dfrac{\partial q_z}{\partial z} + T\left(\dfrac{\partial P}{\partial T}\right)_p\left(\dfrac{\partial v_x}{\partial x} + \dfrac{\partial v_y}{\partial y} + \dfrac{\partial v_z}{\partial z}\right) + \tau_{xz}\left(\dfrac{\partial v_x}{\partial z} + \dfrac{\partial v_z}{\partial x}\right) + \tau_{zy}\left(\dfrac{\partial v_z}{\partial y}\right) \\ q_z = -k_m\frac{\partial T}{\partial z} \end{cases} \quad (15)$$

where k_m is the coefficient of heat conductivity of polymer melt.

In this model, there is no transfer of polymer melt along the z direction, vibration along the z and x directions are used to simulate compression and shear on the polymer melt in the extruder, respectively. The melt film is very thin; therefore, to simplify the deduction, we let $v_z = 0$. Then, eq. (15) is

$$\begin{cases} 0 = \dfrac{\partial q_z}{\partial z} - T\left(\dfrac{\partial P}{\partial T}\right)_p\dfrac{A_1\omega_1\cos(\omega_1 t)}{\pi R^2[H - A_1\sin(\omega_1 t)]} + \tau_{xz}\dfrac{\partial v_x}{\partial z} \\ \dfrac{M}{\pi R^2[H - A_1\sin(\omega_1 t)]}\dfrac{\partial v_x}{\partial t} = \eta\dfrac{\partial^2 v_x}{\partial z^2} - \dfrac{\partial P}{\partial x} \end{cases} \quad (16)$$

Under the impact of a vibration force field, the relationship between the distortion and the stress is related to the relaxation time (λ). From the previous deduction, we know that the shear stress is a function of time t and z. Therefore, the Tanner constitution equation should be used in this model:

$$\tau_{xz} + \lambda \frac{\partial \tau_{xz}}{\partial t} = \eta(\dot{\gamma}) \frac{\partial v_x}{\partial z} \tag{17}$$

$\dot{\gamma}$ is the sheare rate;

$$\eta(\dot{\gamma}) = K\left(\frac{dv_x}{dz}\right)^{n-1} \tag{18}$$

K is the consistency coefficient;

$$K = K'\beta_0\left\{\frac{4n}{\left[3n + 1 + nM_B\eta_0 \times \frac{\omega}{a}\cos\varphi_1\right]}\right\} \times \left[b_1 + b_2 \exp\left(-b_3 \frac{R^3}{R_0^3}\overline{\dot{\gamma}_a}\right)\right] \tag{19}$$

where τ_{xz} is the shear stress in the melt film; n is the power-law index; K' is the consistency coefficient of a Newtonian fluid; β_0 is the modifying coefficient; M_B is the geometry parameter of the capillary rheometer; η_0 is the zero-shear apparent viscosity; a, b_1, b_2, and b_3 are constants determined from the experiments; R_0 is the radius of the capillary; $\overline{\dot{\gamma}_a} = \frac{A\omega}{\delta}$ is the breadth of the nominal shear rate; and φ_1 is the phase angle. Simultaneously, an experiential equation is obtained from the experiment:

$$\cos\varphi_1 = 1 - a_1 \exp(-a_2\omega) \tag{20}$$

where a_1 and a_2 are coefficients of the material determined by the experiment. From refs. 12 and 13, the nominal shear rate can be used to simplify eqs. (17) and (18), so we have

$$\tau_{xz} + \lambda \frac{\partial \tau_{xz}}{\partial t} = \overline{\eta} \frac{\partial v_x}{\partial z} \tag{21}$$

where $\overline{\eta}$ is the equivalent viscocity;

$$\overline{\eta} = K\left(\frac{\overline{V}_x}{h}\right)^{n-1} \tag{22}$$

$\overline{V}_x$ is the equivalent velocity of polymer melt along x direction; and h is the average thickness of melt film.

$$\overline{V}_x = \frac{\sqrt{2}}{2} A_2\omega_2 \tag{23}$$

Combining eqs. (16) and (17), we have

$$\frac{\lambda M}{\pi R^2[H - A_1\sin(\omega_1 t)]}\frac{\partial^2 v_x}{\partial t^2} + \frac{M}{\pi R^2[H - A_1\sin(\omega_1 t)]} \times \left\{1 + \frac{\lambda A_1\omega_1\cos(\omega_1 t)}{\pi R^2[H - A_1\sin(\omega_1 t)]}\right\}\frac{\partial v_x}{\partial t} = \overline{\eta}\frac{\partial^2 v_x}{\partial z^2} - \frac{\partial P}{\partial x} \tag{24}$$

The boundary conditions are

$$\begin{cases} z = 0, & v_x = A_2\omega_2\cos(\omega_2 t) \\ z = h, & v_x = 0 \end{cases} \tag{25}$$

The initial conditions are

$$\begin{cases} t = 0, & v_x = 0 \\ t = 0, & \dfrac{\partial v_x}{\partial t} = 0 \end{cases} \tag{26}$$

Let

$$\rho_m = \frac{M}{\pi R^2[H - A_1\sin(\omega_1 t)]} \tag{27}$$

Inspecting eq. (27) we find that the density (ρ_m) is a function of time t, but a change in the density has little effect on the momentum equation. Therefore, to simplify the deduction, the average density ($\overline{\rho_m}$) is substituted for the dynamic density:

$$\overline{\rho_m} = \frac{M}{\pi R^2 H} \tag{28}$$

Equation (24) can then be changed as follows:

$$\lambda\overline{\rho_m}\frac{\partial^2 v_x}{\partial t^2} + \overline{\rho_m}\left\{1 + \frac{\lambda A_1\omega_1\overline{\rho_m}\cos(\omega_1 t)}{M}\right\}\frac{\partial v_x}{\partial t} = \overline{\eta}\frac{\partial^2 v_x}{\partial z^2} - \frac{\partial P}{\partial x} \tag{29}$$

In this model, the pressure along the z direction is uniform; that is, $\partial P/\partial x = 0$. Moreover, to simplify the deduction, we let

$$\omega = \omega_1 = \omega_2 \tag{30}$$

$$A = A_1 = A_2 \tag{31}$$

The frequency used in a vibration-induced extruder is less than 50 Hz. Under the extrusion conditions, most of the polymer melt's relaxation time is less than 10^2 s; therefore, solving eq. (29) leads to

$$v_x = \frac{k_0}{h}\left[k_1(h - z) + k_2(h - z)^3 + k_3(h - z)^5\right]\cos(\omega t) \tag{32}$$

where

$$k_0 = \frac{72A\omega}{(6 - \omega^2\overline{\rho_m}\lambda h^2/\overline{\eta})^2 + \omega^2\overline{\rho}_m^2 h^4/\overline{\eta}^2} \tag{33}$$

$$k_1 = 1 + [36\omega^2\overline{\rho}_m^2 h^4(1 + \lambda^2\omega^2)/\overline{\eta}^2 - 432\omega^2\overline{\rho_m}\lambda h^2/\overline{\eta}]/2592 \tag{34}$$

$$k_2 = [144\omega^4\overline{\rho}_m^2\lambda^2 h^2/\overline{\eta}^2 - 12\omega^4\overline{\rho}_m^3 h^4\lambda(1 + \lambda^2\omega^2)/\overline{\eta}^3 - 432\omega^2\overline{\rho_m}\lambda/\overline{\eta}]/2592 \tag{35}$$

$$k_3 = [\omega^4\overline{\rho}_m^4 h^4(1+2\lambda^2\omega^2+\lambda^2\omega^2)/\overline{\eta}^4 + 36\omega^2\overline{\rho}_m^2(1+\omega^2\lambda^2)/\overline{\eta}^2 - 12\omega^4\overline{\rho}_m^3 h^2\lambda(1+\lambda^2\omega^2)/\overline{\eta}^3]/2592 \quad (36)$$

Substituting eq. (32) into eq. (21) leads to

$$\tau_{xz} = \frac{k_0\overline{\eta}\left[-k_1 - 3k_2(h-z)^2 - 5k_3(h-z)^4\right](\lambda\cos\omega t + \omega\lambda^2)}{(1+\omega^2\lambda^2)h\lambda} \quad (37)$$

Solving eqs. (37) and (16), we have

$$0 = k_m\frac{\partial^2 T}{\partial z^2} - T\left(\frac{\partial T}{\partial T}\right)_p\frac{A\omega\cos(\omega t)}{\pi R^2[H - A\sin(\omega t)]} + \frac{k_0^2\overline{\eta}\left[-k_1 - 3k_2(h-z)^2 - 5k_3(h-z)^4\right]^2\cos(\omega t)(\lambda\cos\omega t + \omega\lambda^2)}{(1+\omega^2\lambda^2)h^2\lambda} \quad (38)$$

From the Spence–Gilmore state equation for polymer materials, we have

$$(P+C)(V+B) = R'T \quad (39)$$

where C is the pressure constant, V is the volume; B is the specific volume constant, and R' is the gas constant. Substituting eq. (39) into eq. (38), we have

$$k_m\frac{\partial^2 T}{\partial z^2} = (P+C)\frac{A\omega\cos(\omega t)}{\pi R^2[H - A\sin(\omega t)]} - \frac{k_0^2\overline{\eta}\cos(\omega t)(\lambda\cos\omega t + \omega\lambda^2)}{(1+\omega^2\lambda^2)h^2\lambda}[k_1^2 + 6k_1k_2(h-z)^2 + (9k_2^2 + 10k_1k_3)(h-z)^4 + 30k_2k_3(h-z)^6 + 25k_3(h-z)^8] \quad (40)$$

With the boundary conditions

$$\begin{cases} z = 0, & T = T_b \\ z = h, & T = T_m \end{cases} \quad (41)$$

When eq. (40) is solved, an expression for the heat flux from the polymer melt to the solid–melt interface is obtained:

$$-[q_m]|_{z=h} = -k\left.\frac{\partial T}{\partial z}\right|_{z=h} = \frac{k_m(T_b - T_m)}{h} - \frac{(P+C)A\omega\cos(\omega t)}{2\pi R^2[H - A\sin(\omega t)]}h + \frac{k_0^2\overline{\eta}\cos(\omega t)(\lambda\cos\omega t + \omega\lambda^2)k_1^2}{2(1+\omega^2\lambda^2)h\lambda} + \frac{k_0^2\overline{\eta}\cos(\omega t)(\lambda\cos\omega t + \omega\lambda^2)}{(1+\omega^2\lambda^2)\lambda}\left[\frac{1}{2}k_1k_2h + \frac{1}{30}(9k_2^2 + 10k_1k_3)h^3 + \frac{30k_2k_3}{56}h^5 + \frac{25k_3}{90}h^7\right] \quad (42)$$

where q_m is the heat flow of melt.

We let the descending velocity of the solid bed be V_{sz}. From the conservation of energy equation, we have

$$k_s\frac{d^2T}{dz^2} + \rho_s c_s V_{sz}\frac{dT}{dz} = 0 \quad (43)$$

where k_s is the coefficient of heat conductivity of polymer solid; ρ_s is the density of polymer solid; and c_s is the specific heat of the polymer solid. The boundary conditions are

$$\begin{cases} y = h, & T = T_m \\ y = \infty, & T = T_s \end{cases} \quad (44)$$

where T_s is the temperature of polymer solid.

Solving eq. (43) leads to

$$T = (T_m - T_s)\exp\left[\frac{\rho_s c_s V_{sz}}{k_s}(h-z)\right] + T_s \quad (45)$$

The heat flux from solid–melt interface to the solid bed is

$$-[q_{sz}]_{z=h} = k_s\left(\frac{dT}{dz}\right)_{z=h} = \rho_s c_s V_{sz}(T_m - T_s) \quad (46)$$

where q_{sz} is the heat flow of polymer solid along z direction.

In this model, the wall of the barrel is adiabatic, and the growth speed of the melt is equal to the melting speed of the solid bed. Therefore, we have

$$k_m\left(\frac{dT}{dz}\right)_{z=h} - k_s\left(\frac{dT}{dz}\right)_{z=h} = V_{sz}\rho_s\lambda_0 \quad (47)$$

where λ_0 is the latent heat of polymer material.

Figure 2 Photos of the DWZD-500: (a) multidimensional vibrating desk and (b) data capture system. [Color figure can be viewed in the online issue, which is available at wileyonlinelibrary.com.]

Combining eqs. (42), (46), and (47) leads to

$$V_{sz} = \frac{k_m(T_b - T_m)}{h[\rho_s\lambda_0 + \rho_s c_s V_{sz}(T_m - T_s)]} - \frac{(P + C)hA\omega\cos(\omega t)}{2\pi R^2[H - A\sin(\omega t)][\rho_s\lambda_0 + \rho_s c_s V_{sz}(T_m - T_s)]} + \frac{k_0^2\overline{\eta}\cos(\omega t)(\lambda\cos\omega t + \omega\lambda^2)k_1^2}{2(1 + \omega^2\lambda^2)h\lambda[\rho_s\lambda_0 + \rho_s c_s V_{sz}(T_m - T_s)]} + \frac{k_0^2\overline{\eta}\cos(\omega t)(\lambda\cos\omega t + \omega\lambda^2)}{(1 + \omega^2\lambda^2)\lambda[\rho_s\lambda_0 + \rho_s c_s V_{sz}(T_m - T_s)]}\left[\frac{1}{2}k_1k_2h + \frac{1}{30}(9k_2^2 + 10k_1k_3)h^3 + \frac{30k_2k_3}{56}h^5 + \frac{25k_3}{90}h^7\right] \quad (48)$$

Melting mass of the solid bed at a certain time

As shown in Figure 1, the interface between the solid bed and the melt is a taper–platform face, the projection of which along the z coordinate is the equivalent circle face. We let the melting mass per unit time be ΔQ, and the melting mass during time t is Q. Then, from the law of conservation of mass, we have

$$\Delta Q = \pi R^2\rho_s V_{sz}\Delta t \quad (49)$$

or

$$dQ = \pi R^2\rho_s V_{sz}dt \quad (50)$$

Then

$$\int_0^Q dQ = \int_0^t \pi R^2\rho_s V_{sz}dt \quad (51)$$

Substituting eq. (48) into eq. (51), we obtain

$$Q = \frac{k_m\pi R^2\rho_s(T_b - T_m)t}{h[\rho_s\lambda_0 + \rho_s c_s V_{sz}(T_m - T_s)]} - \frac{\pi R^2\rho_s(P + C)h}{2\pi R^2[\rho_s\lambda_0 + \rho_s c_s V_{sz}(T_m - T_s)]}\ln\left[\frac{H - A\sin(\omega t)}{H}\right] + \frac{\pi R^2\rho_s k_0^2\overline{\eta}k_1^2[\sin(2\omega t) + 2\omega t + 4\omega\lambda\sin(\omega t)]}{8\omega h(1 + \omega^2\lambda^2)[\rho_s\lambda_0 + \rho_s c_s V_{sz}(T_m - T_s)]} + \frac{k_0^2\overline{\eta}h[\sin(2\omega t) + 2\omega t + 4\omega\lambda\sin(\omega t)]}{8\omega(1 + \omega^2\lambda^2)[\rho_s\lambda_0 + \rho_s c_s V_{sz}(T_m - T_s)]}\left[k_1k_2 + \frac{1}{15}(9k_2^2 + 10k_1k_3)h^2 + \frac{15k_2k_3}{14}h^4 + \frac{5k_3}{9}h^6\right] \quad (52)$$

EXPERIMENTAL

Apparatus for the experiment

DWZD-500 is the multidimensional vibrating desk designed by Guang-Sheng Zeng used in this study. As shown in Figure 2, it is composed of one moving oil cylinder and two vibrators. The moving oil cylinder can push the piston downward, and the vibrator can move the piston and the hot plate along the z and x directions, respectively. The inside of the hot plate is empty, but cooling water can flow in it. Also, a temperature and pressure sensor is used to capture the corresponding data.

Materials for the experiment

Low-density polyethylene (LDPE; 951- 050, Petrochemicals Co., Ltd., Maoming, China) was used in this study. The physical properties are given in Table I.

TABLE I
Physical Properties of the Solid LDPE (951-050)

ρ_s (kg/m^3)	T_g (°C)	k_s (W m^{-1} °C^{-1})	C_{ps} (kJ kg^{-1} °C^{-1})	λ (kJ/kg)
915	−68	0.335	2.76	129.8

TABLE II
Vibration Parameter Combination for the Hot Plate

		Vibration amplitude				
Viscosity		0	0.5	1.0	1.5	2.0
Vibration frequency	0					
	5					
	10					
	15					
	20					
	25					

Experimental procedure

The lower plate was heated by electricity, and the temperature of the plate was set to 60°C and controlled by the computer, temperature sensors, and cooling water pipes around the barrel and in the plate. After the temperature reached the set value, 50 g of LDPE was pulled into the barrel, and the piston began applying a pressure of 3 MPa. The lower plate and the piston vibrated, as depicted in Figure 1, at the same time with the same vibration parameters. Each new test was run for 5 min with the piston and the hot plate vibration parameters set to different combinations, as listed in Table II. Afterward, the vibration and cooling water was stopped, and the sample was removed. The vibration frequency was adjusted from 0 to 25 Hz with a step size of 5 Hz, and the amplitude was set from 0 to 2 mm with a step size of 0.5 mm. Also, the pressure and temperature data were recorded during the experiments with temperature and pressure sensors. Finally, the mass of the melting polymer extruded form the equipment was weighed and recorded as the melting mass.

RESULTS AND DISCUSSION

The introduction of a vibration force field can speed up the untangling of long molecule chains and enhance friction among molecule chains and molecule chain segments. The polymer solid is continuously broken up, crushed, and rubbed under the influence of the vibration force field. The vibration force improves the melting process of a polymer material. Even without an outside heating source, the polymer material can be melted; ultrasonic welding of plastic is a representative example.

Figure 3 shows a photo of the experimental sample. As shown in Figure 3, the melt first occurred at the interface between the hot plate and the solid bed; finally, a circular melt pool was generated. The melting process was in good agreement with the physical model shown in Figure 1.

Figure 4 shows the melting mass per unit time of the polymer material as a function of the vibration parameters, where A is the amplitude and Q is the melting mass. It was clear that the melting mass increased as the vibration amplitude and frequency increased.

Figure 5 compares the melting mass per unit time (5 min) from the experimental and theoretical calculations (under various combinations of vibration parameters), where E denotes the experimental values and T is the theoretical value. As shown clearly in the E curve of Figure 5, increasing the vibration amplitude and frequency increased the melting mass; this was in good agreement with the calculated results. Furthermore, as shown in Figure 5, although

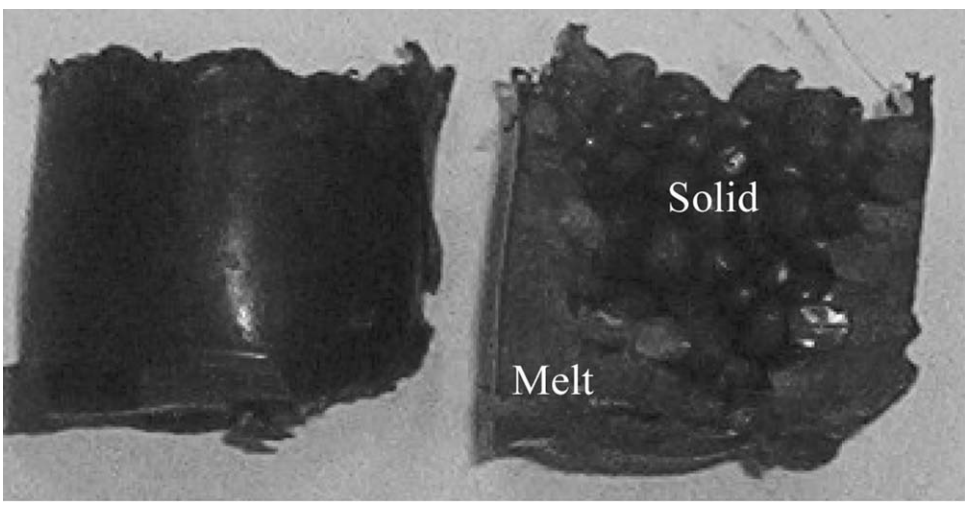

Figure 3 Experimental sample coming from DWZD-500.

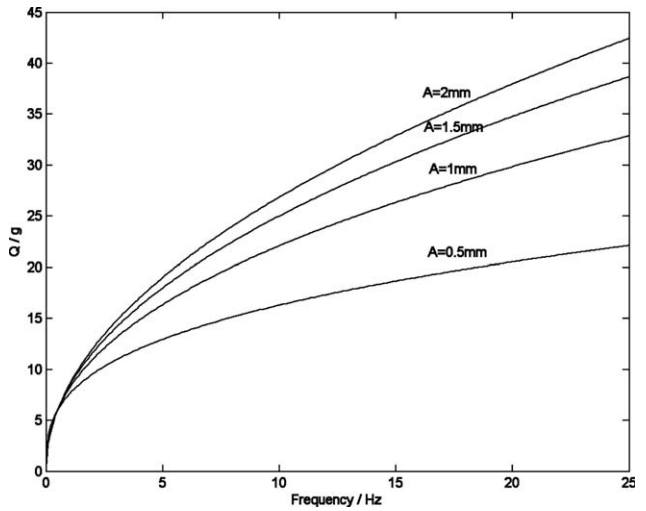

Figure 4 Relationship between the melting mass and the vibration parameters coming from the theoretical model.

the experimental results were very consistent with the theoretical calculation, there were still minor deviations among them, especially in Figure 5(a,b). This was because many assumptions were made to obtain an analytical expression of the melting model, which could not be totally neglected. On the other hand, test error could be another reason for the deviation.

CONCLUSIONS

Through the DWZD-500 multidimensional vibration desk experiment, the melting mechanism was researched deeply, and a reliable physical model was established. Subsequently, the mathematical analytical model was derived by sophisticated mathematical deduction. The results coming from theoretical calculation were in good agreement with those of the experiment, and the following conclusions were obtained:

1. The introduction of the vibration force field sped up the untangling of long molecule chains, decreased the viscosity, and improved the flowability of the polymer melt.
2. The introduction of the vibration force field enhanced the dissipation energy and then

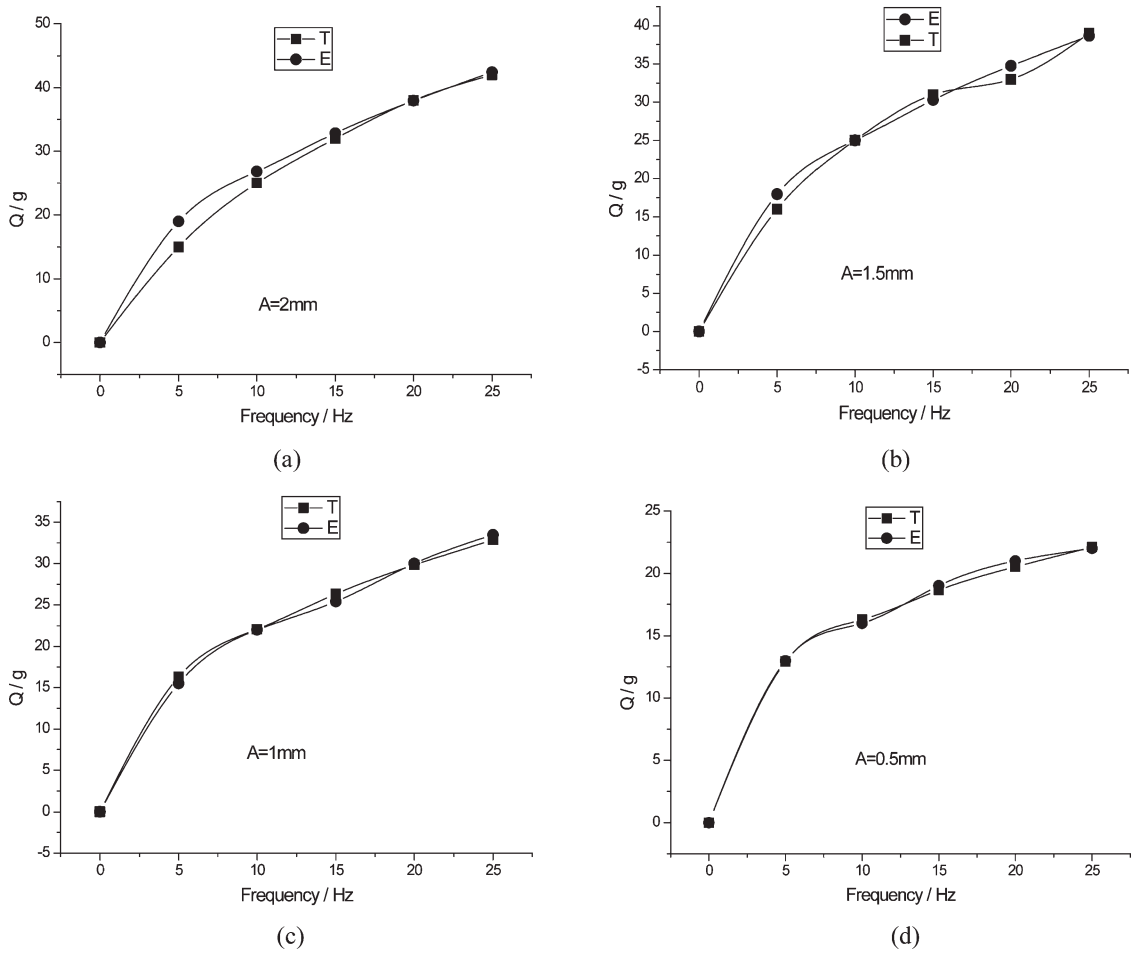

Figure 5 Relationship between the melting mass and the vibration parameters coming from the theory calculation and experiment.

increased the plastication molding rate of the polymer material.

This study will serve as a theoretical basis for the optimum conditions of vibration extruder design and the processing of polymers.

References

1. Maddock, B. H. SPE J 1959, 15, 383.
2. Street, L. F. Int Plast Eng 1961, 1, 289.
3. Tadmor, Z. Polym Eng Sci 1966, 6, 185.
4. Huang, H. X.; Feng, Y. C. Adv Polym Technol 2003, 8, 343.
5. Chris, R. Adv Polym Technol 1998, 15, 135.
6. Qu, J. P.; Zeng, G. S. J Chem Ind Eng (China) 2006, 57, 414.
7. Zeng, G. S.; Qu, J. P. J Chem Ind Eng (China) 2006, 57, 424.
8. Zeng, G. S.; Qu, J. P. Chin J Mater Res 2006, 20, 59.
9. Zeng, G. S.; Qu, J. P. J South China Univ Technol (Nat Sci Ed) 2005, 33, 14.
10. Qu, J. P. Theory and Technic of Polymer Dynamic Plastication Process. Since Press: Beijing, 2005; p 109.
11. Qu, J. P.; Zeng, G. S. J Appl Polym Sci 2006, 100, 3860.
12. Zeng, G. S.; Qu, J. P. J Appl Polym Sci 2007, 104, 2504.
13. Zeng, G. S.; Qu, J. P. J Appl Polym Sci 2007, 106, 1152.
14. Fridman, M. L.; Peshkovsky, S. L. Adv Polym Sci 1993, 90, 41.
15. Fridman, M. L.; Peshkovsky, S. L.; Vinogradov, G. V. Polym Eng Sci 2004, 21, 755.
16. Zeng, G. S.; Qu, J. P. Mater Sci Technol 2008, 16, 235.
17. Zeng, G. S.; Qu, J. P.; He, H. Z.; Jin, G. J Chem Ind Eng 2007, 58, 3158.
18. Zeng, G. S.; Qu, J. P.; He, H. Z.; Jin, G. J Chem Ind Eng 2007, 58, 3164.